

A novel function for the Rab5 effector Rabenosyn-5 in planar cell polarity

Giovanna Mottola^{1,2}, Anne-Kathrin Classen¹, Marcos González-Gaitán^{1,3}, Suzanne Eaton¹ and Marino Zerial^{1,*}

SUMMARY

In addition to apicobasal polarization, some epithelia also display polarity within the plane of the epithelium. To what extent polarized endocytosis plays a role in the establishment and maintenance of planar cell polarity (PCP) is at present unclear. Here, we investigated the role of Rabenosyn-5 (Rbsn-5), an evolutionarily conserved effector of the small GTPase Rab5, in the development of *Drosophila* wing epithelium. We found that Rbsn-5 regulates endocytosis at the apical side of the wing epithelium and, surprisingly, further uncovered a novel function of this protein in PCP. At early stages of pupal wing development, the PCP protein Fmi redistributes between the cortex and Rab5- and Rbsn-5-positive early endosomes. During planar polarization, Rbsn-5 is recruited at the apical cell boundaries and redistributes along the proximodistal axis in an Fmi-dependent manner. At pre-hair formation, Rbsn-5 accumulates at the bottom of emerging hairs. Loss of Rbsn-5 causes intracellular accumulation of Fmi and typical PCP alterations such as defects in cell packing, in the polarized distribution of PCP proteins, and in hair orientation and formation. Our results suggest that establishment of planar polarity requires the activity of Rbsn-5 in regulating both the endocytic trafficking of Fmi at the apical cell boundaries and hair morphology.

KEY WORDS: *Drosophila*, Endocytosis, Planar cell polarity, Wing

INTRODUCTION

Cells in epithelia exhibit a characteristic apicobasal polarity, perpendicular to the plane of the tissue. Their plasma membrane is asymmetrically organized in distinct apical and basolateral domains, differing in protein and lipid composition and in functional properties (Mostov et al., 2003). Additionally, epithelial cells can be polarized along the plane, a form of polarity called planar cell polarity (PCP). The wing of *Drosophila melanogaster* provides an excellent biological system in which to study both forms of epithelial polarity in vivo (Adler, 2002; Eaton, 2003). The larval wing imaginal disc is an epithelial structure that undergoes dramatic morphogenetic changes during pupal metamorphosis: irregularly shaped cells convert into a monolayer of regularly packed hexagonal cells with the acquisition of PCP (Classen et al., 2005). Each cell of the monolayer produces an actin-enriched hair or trichome at its distal-most apical edge pointing towards the distal side of the wing. All hairs in the adult wing are precisely positioned and aligned with each other. Genetic studies in *Drosophila* have identified a 'core' group of proteins that control PCP in several organs and that are highly conserved in vertebrates (Klein and Mlodzik, 2005; Strutt and Strutt, 2005). This group includes transmembrane proteins, such as Frizzled (Fz), Flamingo (Fmi; also known as Starry night) and Strabismus (Stbm; also known as Van Gogh), and peripheral membrane proteins, such as Dishevelled

(Dsh), Prickle and Diego. In the pupal wing, shortly before pre-hair emergence, PCP proteins adopt an asymmetric proximodistal (PD) subcellular distribution at the apical cell boundaries of epithelial cells: Stbm and Prickle localize to the proximal cell boundaries; Fz, Dsh and Diego to the distal; whereas Fmi is present on both sides. Additionally, all of these proteins might interact both intra- and inter-cellularly at the apical cell boundaries and function interdependently. Mutations in any of them affect the apical recruitment or the PD polarity of all other PCP proteins, leading to global misalignment of hair polarity, as well as to defects in hexagonal packing geometry (for reviews, see Adler, 2002; Klein and Mlodzik, 2005; Strutt and Strutt, 2005; Zallen, 2007) (Classen et al., 2005). The asymmetric localization and the ability to form stable complexes appear to lead to asymmetric intercellular signalling specifying the site of hair initiation. Such signalling is thought to depend on long-range patterning cues along the PD wing axis, involving the upstream cadherin molecules Dachshous (Ds) and Fat, and the Golgi-protein Four-jointed (Fj) (Saburi and McNeill, 2005; Strutt and Strutt, 2009).

Over the past few years, intracellular membrane trafficking has emerged as a crucial regulator of PCP in the *Drosophila* wing. Functional blockade of Dynamin and Rab11, which are required for the scission of endocytic vesicles from and the recycling of endocytic cargo to the plasma membrane, respectively, disrupts PCP-dependent hexagonal repacking (Classen et al., 2005). Intracellular vesicles double-positive for Fz-GFP and Fmi moving preferentially towards distal boundaries were detected by live-cell imaging before the localization of PCP proteins to the PD cortex (Shimada et al., 2006). In fixed tissue, blockade of trafficking to late endosomes resulted in intracellular accumulation of Fmi and Fz on early endosomes (Strutt and Strutt, 2008). Therefore, endocytic trafficking has been proposed to regulate the localization and signalling asymmetries of PCP proteins and to establish PCP in the tissue.

¹Max Planck Institute of Molecular Cell Biology and Genetics, Pfotenhauerstrasse 108, 01307 Dresden, Germany. ²Dipartimento di Biochimica e Biotecnologie Mediche, University of Naples 'Federico II', Via S. Pansini 5, 80131 Naples, Italy. ³Departments of Biochemistry and Molecular Biology, University of Geneva, Geneva 1211, Switzerland.

*Author for correspondence (zerial@mpi-cbg.de)

Elucidating the molecular mechanisms underlying polarized cell trafficking is thus an important step towards the understanding of epithelial biogenesis and maintenance. In this respect, small GTPases of the Rab family play a key role. Among these proteins, Rab5 is an evolutionarily conserved, master regulator of endocytosis (Zerial and McBride, 2001). It regulates the tethering and fusion of endocytic vesicles with early endosomes and homotypic early endosome fusion (Bucci et al., 1992; Gorvel et al., 1991), the motility of endosomes along actin and microtubules (Hoepfner et al., 2005; Nielsen et al., 1999; Pal et al., 2006), and signalling (Barbieri et al., 2000; Lanzetti et al., 2000; Miaczynska et al., 2004). Rabenosyn-5 (Rbsn-5) is one of the best-characterized Rab5 effectors, highly conserved from yeast to mammals (Nielsen et al., 2000). Rbsn-5 associates with early endosomes in a Rab5- and phosphatidylinositol 3-phosphate [PtdIns(3,4,5)P₃]-dependent manner, and interacts with multiple endosomal proteins. It binds to the Sec1-like protein VPS45, which interacts with endosomal syntaxins (Bryant et al., 1998; Pevsner et al., 1996; Tellam et al., 1997). In addition to Rab5, it also binds to Rab4 [through a distinct binding site (de Renzis et al., 2002)] and to EHD1/RME-1 (Naslavsky et al., 2004), two regulators of the recycling route (Grant et al., 2001; Iwahashi et al., 2002; Lin et al., 2001; van der Sluijs et al., 1992). Consistent with these interactions, Rabenosyn-5 is required for cargo recycling to the plasma membrane (Naslavsky et al., 2004). Moreover, it also regulates sorting of cargo for lysosomal degradation (Nielsen et al., 2000). Whereas Rabenosyn-5 has been investigated in non-polarized cells, its function in polarized epithelial cells is, to date, largely unknown. To address this problem, and given the functional conservation of Rabenosyn-5 in evolution, we explored the role of this protein in the development of *Drosophila* wing epithelia.

MATERIALS AND METHODS

Fly stocks and genetics

Control and driver strains (Bloomington *Drosophila* Stock Center, Indiana University); *UAS-GFP**Rab5* (Wucherpfennig et al., 2003), *Sp/CyO;UAS-Fmi* (Usui et al., 1999); *fmi*¹⁹², *FRT42* [T. Wolff (Rawls and Wolff, 2003)]; *UAS-Fz* (Adler et al., 1997).

We identified the Rbsn-5 gene (*CG8506* on FlyBase) by sequence comparison to the human Rabenosyn-5 gene (Nielsen et al., 2000) and cloned it from the cDNA LD29542. However, during the preparation of this manuscript, the *Drosophila* Rbsn-5 gene was reported (Tanaka and Nakamura, 2008). Rbsn-5, *DmVps45* (*CG8228*) and *Past1* (*CG6148*) cDNAs were obtained from the Berkeley *Drosophila* Genome Project (BDGP).

To generate *rbsn*³⁴ and *rbsn*²²⁰ mutants, imprecise excision was performed using the P-element GE11609 (GenExel). *rbsn*³⁴ is a 705-bp deletion starting 80-bp upstream of the 5'-UTR and covering the ATG and 372 bp of the first exon. *rbsn*²²⁰ is a 1518-bp deletion starting 83-bp upstream of the 5'-UTR and covering the ATG, the first exon and 455 bp of the second exon. Both deletions do not extend into the gene *CG8552*, positioned 235 bp upstream of the 5' UTR region. To test the specificity of the lethality phenotype observed, we used the stock *In(1 w^{m4h}, y¹; Df(2L)TE29Aa-11/CyO*). For rescue experiments, the GFP-tagged Rbsn-5 protein was expressed in transgenic flies under the control of the ubiquitous *Tubulin* promoter (Marois et al., 2006). In the rescue experiment, homozygous *rbsn*³⁴ or *rbsn*²²⁰ expressing GFP*Rbsn-5* (genotype *w; rbsn*^{-/-}; *Tub-GFP**Rbsn-5/TM3Sb*) were generated and developed normally until adult stage. Adult wings of rescued flies did not show any phenotype.

Mutant clones were generated using the FLP/FRT technique (Xu and Rubin, 1993). For *rbsn*³⁴ clones, females of the genotype *y,w,hsp70-FLP;rbsn*³⁴, *FRT40A/CyO* were crossed to *w¹¹¹⁸;UbiGFP(S65T)nls,FRT40A/CyO* males. For the control cross, females of the genotype *y,w,hsp70-FLP;Gbe/+* were crossed to *w¹¹¹⁸;UbiGFP(S65T)nls,FRT40A/CyO* males. Crosses were grown at 25°C. Then first/second instar larvae were heated for 1 hour at 37°C and transferred at 18°C.

*fmi*¹⁹² clones were generated as previously described (Rawls and Wolff, 2003; Usui et al., 1999) and grown at 18°C. In *Fmi*, *Stbm* and *Fz* overexpression experiments, pupae were dissected at 26 hours after puparium formation (APF), before the establishment of PD polarity in the whole wing, in order to detect at best Rbsn-5 recruitment to the apical cell boundaries. Staging of pupal wing development at 18°C and 25°C was performed as described (Classen et al., 2008).

In vitro binding assay

Proteins were in vitro translated and labelled by ³⁵S-methionine using a TnT-coupled transcription-translation kit (Promega). Five µl of the *DmVps45* or *Past1* proteins were incubated with 30 µl of glutathione-Sepharose beads loaded with GST or GST-Rbsn-5. Bound proteins were eluted from the beads and analysed by SDS-PAGE and autoradiography.

GST fused to full-length *Drosophila* Rab5, Rab4, Rab7 and Rab11 proteins were expressed using pGEX-6P-1 (Pharmacia Biotech). GTP/GDP binding assays were performed as previously described (Christoforidis et al., 1999) by incubating 5 µl of the translated Rbsn-5 protein with 30 µl of glutathione-Sepharose beads (Pharmacia Biotech) loaded with GST-Rab5, GST-Rab4, GST-Rab7 or GST-Rab11, in presence of either GDP or GTPγS. Bound proteins were eluted from the beads, separated by SDS-PAGE and analysed by autoradiography. GST-Fmi and GST-Stan were used as previously described (Wasserscheid et al., 2007).

In all the GST pull-down experiments, the loading control (L) represents 20% of the total amount of in vitro translated proteins used for incubation.

Generation of antibodies

Full-length Rbsn-5 and Rab5 were expressed in *Escherichia coli* as GST fusion proteins using pGEX-6P-1 (Pharmacia Biotech). The purified fusion proteins were injected into rabbit and bled out. Rabbit antisera were pre-absorbed with glutathione-Sepharose beads loaded with GST, in order to remove anti-GST antibodies, and then directly used for immunoblotting and fluorescence analysis.

A polyclonal antiserum against Rbsn-5 was generated by immunizing rabbits with the SGNPFDSDEDQSSASC synthetic peptide corresponding to the 16 N-terminal amino acid residues of Rbsn-5 (Eurogentec, Belgium) and affinity purified as described (Nielsen et al., 2000).

Specificity of the antisera was verified by western blot analysis of extracts from *Drosophila* S2 cells, pupae (Fig. 1D) or all developmental stages (not shown).

Immunofluorescence and antibodies

Antibody staining on wing imaginal discs and pupal wings was performed as previously described (Classen et al., 2005; Strigini and Cohen, 2000), by using PBS 0.01% Triton X-100. Dextran uptake was performed as previously described (Entchev et al., 2000). Confocal images were acquired at 40×, 63× and 100× magnification on a Meta Zeiss Confocal Microscope. Confocal sections were spaced 0.4 µm apart.

Primary antibodies were: mouse anti-Fmi [1:20 (Usui et al., 1999)] and rat anti-E-Cad [1:100 (Oda et al., 1994)] from the Developmental Studies Hybridoma Bank (DSHB, University of Iowa, USA); rabbit anti-Fz (1:300) (Bastock and Strutt, 2007); rat anti-Stbm (Strutt and Strutt, 2008); rabbit anti-Stbm (1:500) (Rawls and Wolff, 2003); rat anti-Dsh (1:1000) (Yanagawa et al., 1995); guinea pig anti-Hrs (1:1000) (Lloyd et al., 2002); rabbit anti-Rab7 (1:100); mouse anti-GFP (Molecular Probes, Eugene, OR, USA). Secondary antibodies were goat anti-mouse and anti-rabbit coupled to Alexa 488, Alexa 546 (Molecular Probes) or Cy5 (Jackson ImmunoResearch Laboratories). Rhodamine-conjugated Phalloidin (Molecular Probes) was used to stain actin filaments.

RESULTS

Characterization of the *Drosophila* orthologue of human Rabenosyn-5

A single orthologue of human (*Hs*) Rabenosyn-5, *CG8506*, has been identified (Tanaka and Nakamura, 2008). The *CG8506* gene encodes a protein of 505 amino acid residues (aa), named Rbsn-5, sharing with *Hs*Rabenosyn-5 (Fig. 1A) the N-terminal C₂H₂ and

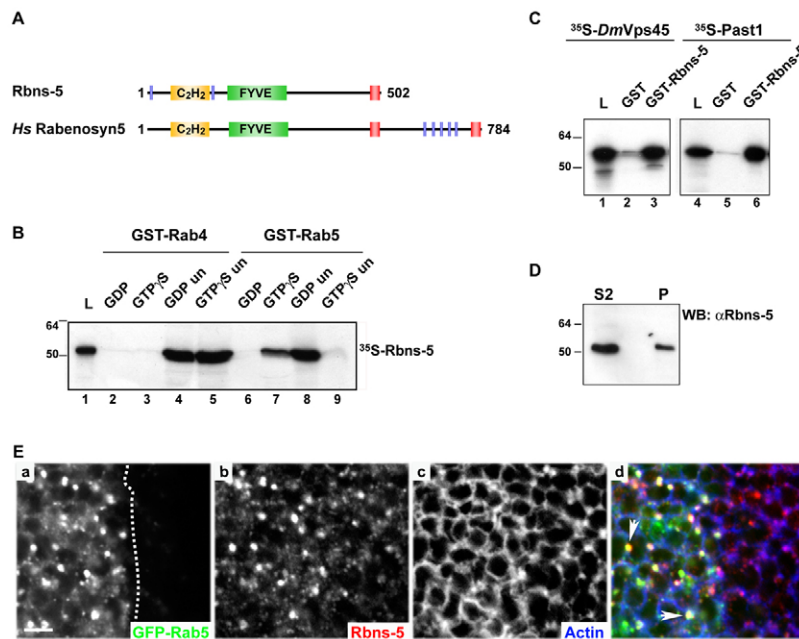


Fig. 1. Characterization of Rbsn-5. (A) Comparison between *Drosophila* (*Rbsn-5*) and human (*Hs*) Rabenosyn-5. Rbsn-5 and *Hs*Rabenosyn-5 share the FYVE finger (FYVE, green rectangle), zinc finger (C₂H₂, yellow rectangle) and NPF (blue bars) motifs. The C-terminus of Rbsn-5 (aa 447-491, red rectangle) has homology to both the Rab4-binding site (aa 440-503) and the Rab5-binding site (aa 728-784) of *Hs*Rabenosyn-5. (B) Rbsn-5 binds Rab5 in a GTP-dependent manner but not Rab4. Glutathione-Sepharose beads loaded with GST-Rab4-GDP (lane 2), GST-Rab4-GTPγS (lane 3), GST-Rab5-GDP (lane 6) or GST-Rab5-GTPγS (lane 7) were incubated with ³⁵S-methionine-labelled in vitro-translated Rbsn-5. Bound proteins were eluted from the beads and analyzed together with the loaded sample (lane 1) by SDS-PAGE and autoradiography. GDP-un and GTPγS-un are the unbound proteins (lanes 4,5,8,9). (C) Rbsn-5 interacts with *Dm*Vps45 and Past1 (EHD1/RME-1 orthologue). Glutathione-Sepharose beads loaded with GST (lanes 2,5) or GST-Rbsn-5 (lanes 3,6) were incubated with ³⁵S-methionine-labelled in vitro-translated *Dm*Vps45 (lanes 2,3) or Past1 (lanes 5,6). Bound proteins were eluted from the beads and analyzed together with the loaded samples (lanes 1,4) by SDS-PAGE and autoradiography. (D) Rbsn-5 detected by western blot of S2 cell (S2) and pupal (P) extracts with a polyclonal antiserum raised against the full-length protein. Molecular mass (kDa) is indicated for B-D. (E) Rbsn-5 localizes to Rab5-positive early endosomes. Wing imaginal discs overexpressing GFP-Rab5 (a, green, on the left of the dashed line) stained with anti-Rbsn-5 antibody (b, red) and Rhodamine-phalloidin (c, blue). Arrowheads indicate colocalization of Rab5 and Rbsn-5 on endosomes (d). A single apical confocal section is shown. Genotype *en-gal4/UAS-GFP-Rab5*. Scale bar: 10 μm.

the FYVE zinc fingers, responsible for endosomal targeting via the interaction with Rab5 and PtdIns(3,4,5)P₃, respectively (Nielsen et al., 2000). In addition, the C-terminus of Rbsn-5 (aa 447-491; Fig. 1A, red rectangle) presents significant homology to both the central (aa 440-503) and the C-terminal region (aa 728-784) of *Hs*Rabenosyn-5, containing a Rab4-binding site (Eathiraj et al., 2005) and a second high-affinity Rab5-binding site (de Renzis et al., 2002), respectively. Rbsn-5 has two NPF motifs in the N-terminus (aa 4-6 and 68-70) instead of the C-terminal NPF motifs (Fig. 1A, blue bars) binding EHD1/RME-1 in *Hs*Rabenosyn-5 (Naslavsky et al., 2004).

To explore the functional conservation of Rbsn-5, we tested its ability to bind the *Drosophila* counterparts of the human interacting proteins. First, GST-Rab5, -Rab4, -Rab7 and -Rab11 fusion proteins immobilized on glutathione-Sepharose beads were loaded with GDP or GTPγS and incubated with in vitro translated Rbsn-5 (see Materials and methods). Rbsn-5 specifically bound to only Rab5 in a GTPγS-dependent manner (see Fig. 1B, lane 7) (see also Morrison et al., 2008; Tanaka and Nakamura, 2008). Rbsn-5 was also able to bind *Hs*Rab5:GTPγS, but not *Hs*Rab4:GTPγS (data not shown). As a control, *Hs*Rabenosyn-5 was shown to bind to both Rab5:GTPγS and Rab4:GTPγS (data not shown) (de Renzis et al., 2002). Therefore, Rbsn-5 displays biochemical properties of a Rab5, but not a Rab4, effector.

Second, we tested the interaction of Rbsn-5 with the *Drosophila melanogaster* (*Dm*) orthologues of *Hs*Vps45 and EHD1/RME-1 (*CG8228* and *CG6148*, named Past1 by the FlyBase Consortium). In vitro translated *Dm*Vps45 and Past1 bound to GST-Rbsn-5 (Fig. 1C, lanes 3 and 6) but not to GST alone (Fig. 1C, lanes 2 and 5), indicating that the interactions with components of the SNARE and recycling machinery reported for *Hs*Rabenosyn-5 are conserved in its fly orthologue.

To investigate the intracellular localization of endogenous Rbsn-5, we generated two rabbit polyclonal anti-sera (see Materials and methods) that recognized a band of the expected molecular mass (~55 kDa, Fig. 1D) and of similar mobility to in vitro translated Rbsn-5 (compare Fig. 1D with 1B) by western blot analysis. To determine whether Rbsn-5 is recruited to Rab5-positives early endosomes in vivo, we analyzed its intracellular distribution by immunofluorescence microscopy in wing imaginal discs expressing GFP-Rab5 (Entchev et al., 2000). The anti-full-length Rbsn-5 serum detected the endogenous protein, and its specificity was demonstrated by: (1) loss of staining in Rbsn-5 null mutant clones (see Fig. S1 in the supplementary material); and (2) strong signal on endosomes enlarged upon GFP-Rab-5 overexpression (Fig. 1E,a-d, arrows).

Altogether, the combination of bioinformatics, biochemical and morphological studies supports the idea that Rbsn-5 is the fly orthologue of *Hs*Rabenosyn-5.

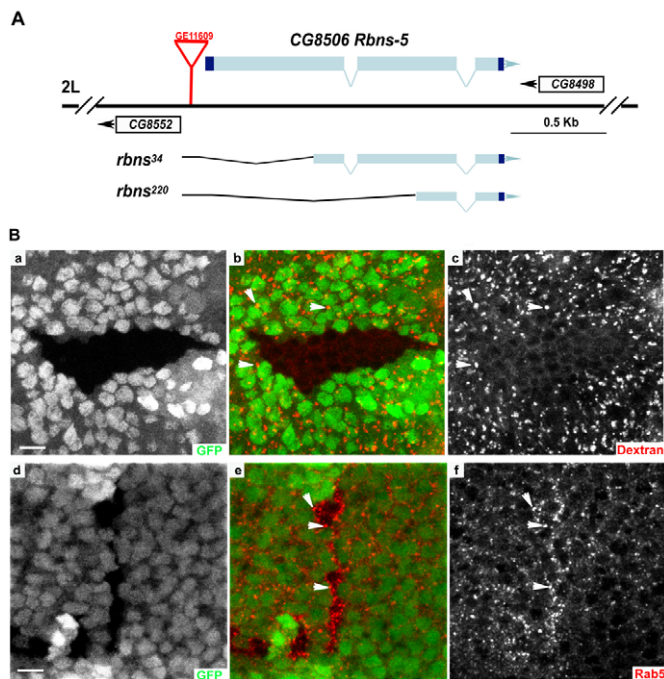


Fig. 2. *rbsn*³⁴ alters endocytosis. (A) Genomic organization of CG8506 *Rbsn-5* (transcript, light blue; 5' and 3' UTR, dark blue; arrow, 3' direction); flanking genes (CG8552 and CG8498); and the transposable element (GE11609, red) used to generate the 0.7 kb and 1.5 kb deletions (*rbsn*³⁴ and *rbsn*²²⁰). (B) Decrease in the number of dextran-labelled endocytic vesicles (red, arrowheads) in *rbsn*³⁴ mutant cells (absence of GFP, green), compared with in wild-type cells (GFP, green) in the wing imaginal disc. A projection of two confocal sections is shown. (Bd-f) Intracellular accumulation of Rab5 (f, red) in *rbsn*³⁴ clones in the wing imaginal disc. Projection of four single confocal sections is shown. Scale bar: 10 μ m.

Rbsn-5 regulates endocytosis in *Drosophila*

To explore the role of Rbsn-5 during development, two distinct deletions in the Rbsn-5 CG8506 gene were generated by imprecise excision: *rbsn*³⁴, having the 5'-UTR, the first ATG codon and almost the entire first exon deleted; and *rbsn*²²⁰, with a larger deletion extending to almost the end of the second exon (Fig. 2A). The two deletions exhibited similar behaviours: zygotic *rbsn*³⁴ and *rbsn*²²⁰ mutants died during the first instar larva stage. Consistent with previous results (Tanaka and Nakamura, 2008), maternal/zygotic *rbsn*³⁴ or *rbsn*²²⁰ mutants died early during embryogenesis. Heterozygotes of *rbsn*³⁴ or *rbsn*²²⁰ over the deficiency *Df(2L)TE29Aa-11*, which deletes the entire Rbsn-5 gene, died early during development. The zygotic lethality of both *rbsn*³⁴ and *rbsn*²²⁰ could be rescued to viability by expressing GFP-tagged Rbsn-5 under control of the ubiquitous Tubulin promoter (data not shown). Rbsn-5 protein was totally absent in *rbsn*³⁴ clones, as verified by immunofluorescence analysis in pupal wings (see Fig. S1 in the supplementary material). These data suggest that both *rbsn*³⁴ and *rbsn*²²⁰ behave as null, rather than hypomorphic, alleles. In subsequent experiments we focused mainly on *rbsn*³⁴.

To investigate the role of Rbsn-5 in endocytic transport, we performed a Texas Red-dextran endocytosis assay on wing imaginal discs containing *rbsn*³⁴ clones (Fig. 2B, panels a-c). In GFP-positive wild-type cells, the fluorescent tracer labelled punctuate cytoplasmic structures (white arrows), corresponding to early and late endosomes (Entchev et al., 2000). In the *rbsn*³⁴ clone

(defined by the absence of GFP), the number of dextran-labelled endocytic structures was strikingly reduced, confirming the requirement of Rbsn-5 for endocytosis (Tanaka and Nakamura, 2008).

Interestingly, in *rbsn*³⁴ clones Rab5 accumulated in several brighter and, occasionally, larger vesicles (Fig. 2B,d-f, arrows). This occurred also in the pupal wing, mainly at the apical side of the epithelium (see below, Fig. 7B,C). Although to a lesser extent, Hrs, a marker of multivesicular bodies (Raiborg et al., 2001) (Fig. 7B,g,k), and Rab7, a marker of late endosomes (Marois et al., 2006) (not shown), also accumulated in *rbsn*³⁴ clones. No intracellular accumulation was detected (data not shown) for the Golgi protein Lava lamp (Sisson et al., 2000). These alterations of the endocytic machinery resemble those induced upon impairment of recycling to the plasma membrane (Cormont et al., 2001; Deneka et al., 2003; Sommer et al., 2005) and are thus compatible with a role of Rbsn-5 in sorting and recycling from early endosomes, as shown in mammalian cells (de Renzis et al., 2002; Naslavsky et al., 2004; Nielsen et al., 2000).

Hexagonal packing, PD polarity of PCP proteins and hair defects in *Rbsn-5* mutant clones

Adult wings containing either *rbsn*³⁴ (Fig. 3A) or *rbsn*²²⁰ (not shown) clones showed patches of tissue with defects characteristic of mutations in PCP genes (Klein and Mlodzik, 2005). Instead of pointing towards the distal side of the wing, hairs were deflected from the PD axis and oriented towards either the posterior or anterior margin (Fig. 3A). Occasionally, cells within the presumed clone had doubled or shorter hairs (Fig. 3A, black arrowheads). Consistently, in pupal wing at pre-hair initiation, cells within *rbsn*³⁴ clones displayed emerging trichomes that were misoriented, pointing away from the clone, (Fig. 3B,a,d,g) or shorter, possibly due to an impairment/delay of hair outgrowth (Fig. 3B,g; red arrowheads). In larger clones, which we found in the distal region of the pupal wing, such impairment in hair formation and elongation was more evident (see Fig. S2A in the supplementary material). Moreover, all defects manifested predominantly in the proximal regions of large *rbsn*³⁴ clones (Fig. 3B,d,g; see also Fig. S2A in the supplementary material). We also observed doubled trichomes in smaller clones (in >4% mutant cells; Fig. 3B,a; red arrowheads) and, rarely (in >2% mutant cells), trichomes emerging from the cell center (Fig. 3B,i; arrowheads). Because these defects were absent in adult wings of rescued flies (data not shown) but were detectable upon overexpression of Rbsn-5 (not shown), they are most likely due to specific alterations of Rbsn-5 function.

PCP mutants alter both the orientation of hair outgrowth and the packing geometry in the pupal wing (Classen et al., 2005). In *rbsn*³⁴ clones, cells failed to acquire the expected hexagonal shape, and Fmi was still cortical and asymmetrically localized, but not always at the PD sites (Fig. 3B,e,h; green asterisks; see also Fig. S2B in the supplementary material). Such defects were also more pronounced in the proximal side of *rbsn*³⁴ clones, where sometimes Fmi was uniformly localized to all cell interfaces (Fig. 3B,h; white asterisks), and was already detectable before pre-hair initiation (see Fig. S3C,G,K,O in the supplementary material). In larger clones, Fmi accumulated along the clone border at the interface between *rbsn*³⁴ and wild-type cells (Fig. 3B,h; see also Fig. S3G,O in the supplementary material, arrowheads), ignoring the normal PD axis. The PD distribution of the proximal PCP protein Stbm and of the distal PCP proteins Fz and Dsh was similarly perturbed (see Fig. S3 in the supplementary material).

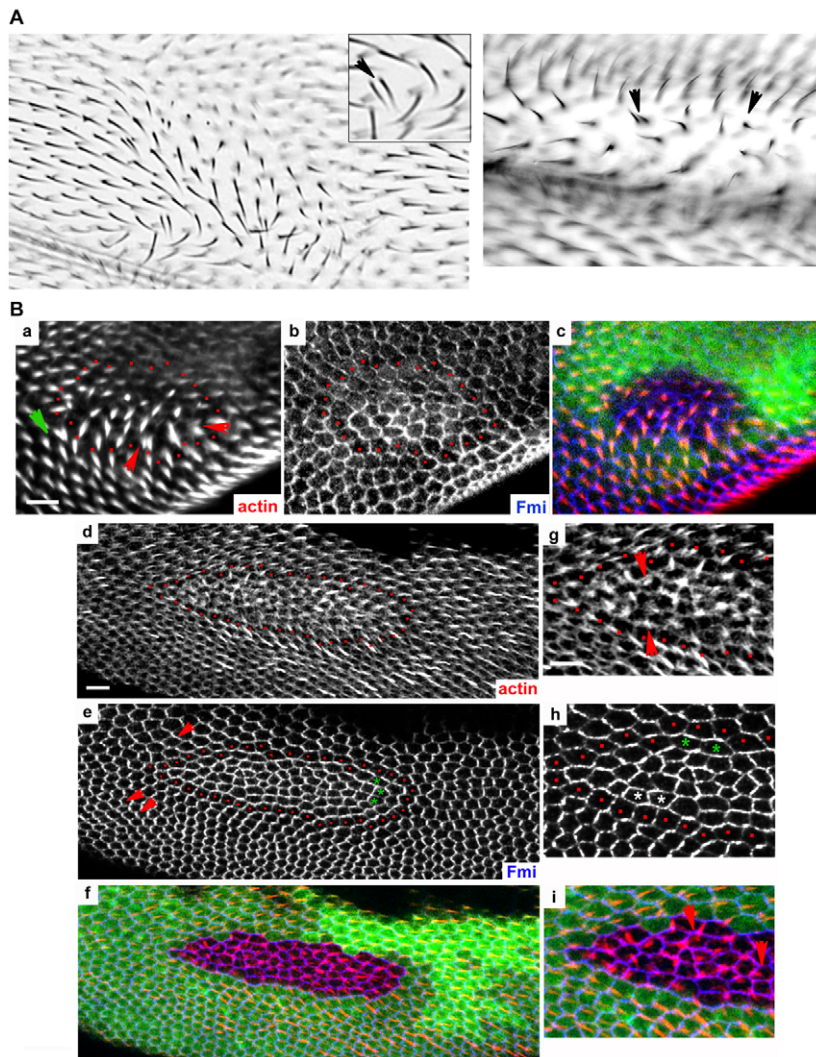


Fig. 3. *rbsn*³⁴ affects hexagonal packing, PD polarity, and hair orientation and formation. (A) Two examples of adult wing containing *rbsn*³⁴ clones. Double or tiny hairs are indicated by black arrowheads. (B a-i) *rbsn*³⁴ clones in the pupal wing [68 hours after puparium formation (APF) at 18°C], indicated by the absence of GFP (green), stained for actin (red) and Fmi (blue). Red arrowheads show: in a, double hairs inside the clone; in e, the Fmi zig-zag pattern oriented obliquely rather than orthogonally to the proximodistal (PD) axis in an area proximal to the clone; in g, shorter hairs; and, in i, trichomes originating from the cell center. Green arrow in a indicates the weak proximal non-autonomy of trichome orientation. White asterisks show cells where Fmi is uniformly present on all cell boundaries; green asterisks indicate a cell in which Fmi is still asymmetrically localized but not at the PD sites. Red dots outline cells abutting the *rbsn*³⁴ clone. (g-i) Higher magnification of the left-proximal part of the clone shown in panels d-f. Scale bar: 10 μm. Distal is right, proximal left.

The overall level of Fmi at the apical cell boundaries was mainly unchanged inside *rbsn*³⁴ clones compared to wild-type surrounding cells. We noticed that mutant cells had a narrower apical cross section, characteristic of vein cells, in ~25% of *rbsn*³⁴ clones, and that such clones were usually adjacent to veins areas and positioned at the pupal wing border. Fmi, other PCP proteins (see Fig. S2B and S3B,C in the supplementary material) and the junctional protein E-Cadherin (E-Cad, not shown) accumulated at the cell boundaries. The localization of E-Cad at the cell junctions was not significantly perturbed (not shown), excluding a general disruption of apicobasal polarity. Reduced apical cross-sectional area is also characteristic of vein cells. Interestingly, adult wings containing *rbsn*³⁴ clones often showed patches of extra or thickened wing veins (not shown). It is possible that *rbsn*³⁴ cells might differentiate into vein cells.

PCP proteins have also been implicated in cell-to-cell propagation of polarity information to establish PD orientation throughout the wing tissue. Consequently, mutations in PCP proteins often show cell non-autonomous effects, i.e. disruption of hair orientation in mutant cells also affects surrounding wild-type cells (for reviews, see Adler, 2002; Klein and Mlodzik, 2005; Strutt and Strutt, 2005; Zallen, 2007). We observed a weak proximal non-autonomy in trichome polarity, such that in proximal cells nearby *rbsn*³⁴ clones trichomes point away from the clone (Fig. 3B,a; see

also Fig. S2A in the supplementary material, green arrowheads), and hexagonal packing and PD domain orientation were also altered, with Fmi running diagonally rather than orthogonally to the PD axis (Fig. 3B,e; see also Fig. S2B in the supplementary material, red arrowheads). Multi-haired cells abutting the *rbsn*³⁴ clone occasionally appeared (Fig. 3B,a). In the first row of wild-type cells adjacent to the *rbsn*³⁴ clone, PCP proteins lost the normal PD orientation and re-aligned according to the orientation of the clone boundary (Fig. 3B,h; see also Fig. S3G in the supplementary material, cells marked with red dot). However, shorter and tiny trichomes were detected only inside the mutant clones. Based on these observations, we conclude that Rbsn-5 is necessary cell-non-autonomously for hexagonal packing, alignment of the PD domains and hair orientation, and is required cell autonomously for hair formation.

Cortical localization and proximodistal polarity of Rbsn-5 during wing development

The defects observed in *rbsn*³⁴ clones prompted us to re-examine the localization of Rbsn-5 in pupal wings during hexagonal cell packing and PCP establishment. Rbsn-5 was always enriched in the apical side of the wing epithelium throughout pupal development (Fig. 4) but was redistributed within the plane of the membrane over time. In pre-pupal wings (Fig. 4A-C), when cells are packed irregularly and

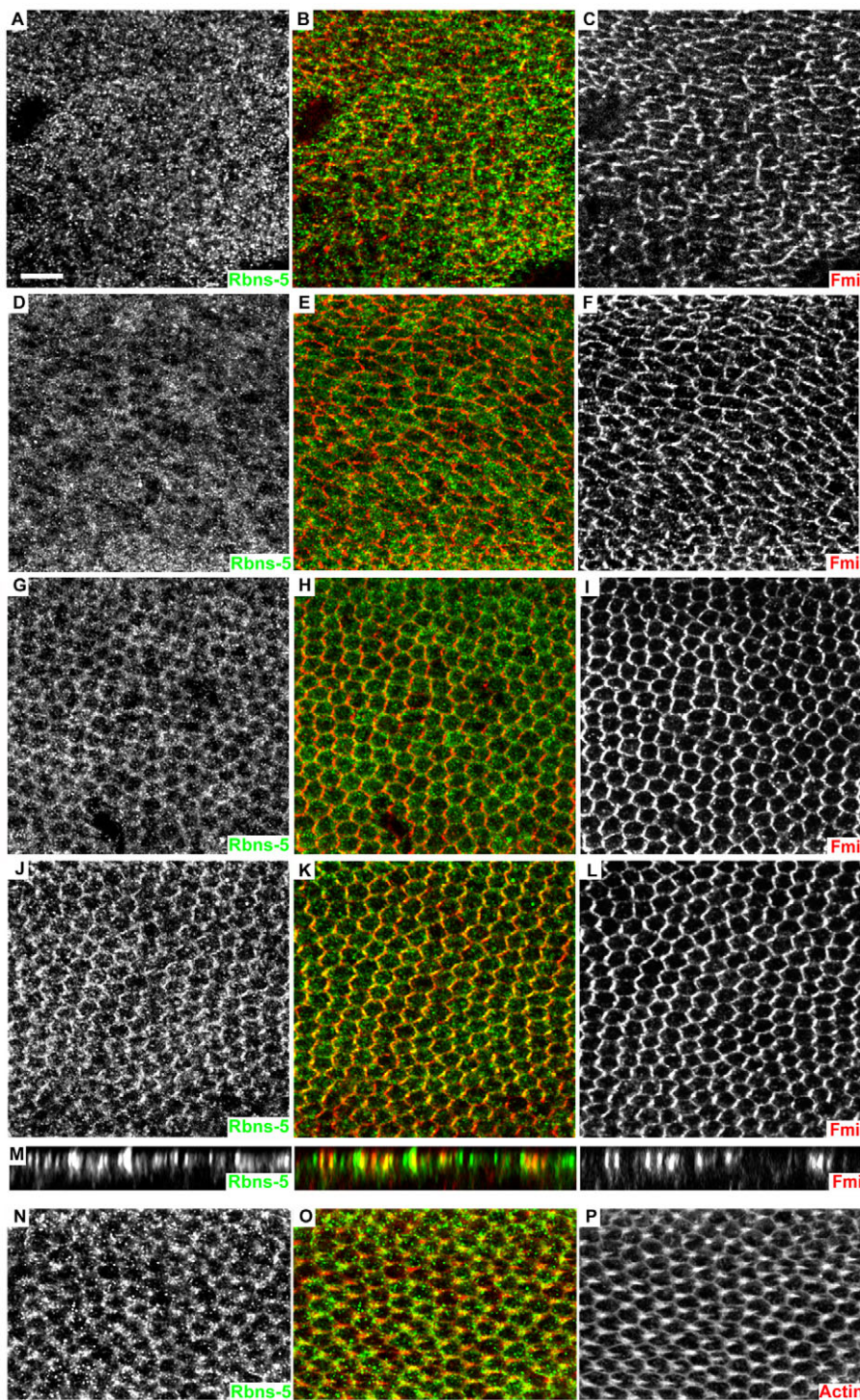


Fig. 4. Rbsn-5 displays a PCP distribution. (A-M) Rbsn-5 (green) and Fmi (red) distribution in pupal wings at 25°C at 6 hours (A-C), 20 hours (D-F), 26 hours (G-I) and 30 hours (J-L) APF; (M) orthogonal section of panels J-L. (N-P) Pupal wing at 32-34 hours APF stained for Rbsn-5 (green) and actin (red). Projections of all apical confocal sections show Fmi staining. Distal is right, proximal left. Scale bar: 10 μ m.

PCP proteins are not uniformly PD oriented, although adjacent cells display coordinated PD polarity (Classen et al., 2005) (Fig. 4C), Rbsn-5 exhibited a punctuate intracellular staining. However, in the course of hexagonal packing and redistribution of Fmi at the apical cell boundaries, Rbsn-5 became progressively more enriched along the cortex, although it was still present in the cytoplasm (Fig. 4D-I). Once hexagonal packing was completed and PD polarity of Fmi fully established in the whole wing, Rbsn-5 at the apical cell cortex preferentially aligned along the PD boundaries (Fig. 4J-L). Such asymmetric distribution resembled (albeit it was less evident) the zig-zag pattern on the epidermal plane characteristic of Fmi (Usui et al.,

1999) and other PCP proteins (Uemura and Shimada, 2003). Indeed, Rbsn-5 retained a vesicular cytoplasmic pattern. Its cortical localization was not always apparent in all areas of the wing and was only detected for a limited period of time, before the onset of trichome outgrowth. Nevertheless, the cortical localization and PD redistribution of Rbsn-5 were specific as it was lost in *rbsn*³⁴ clones (see Fig. S1A-C in the supplementary material, arrowheads). Although Rab5 also localized along the cortex (Fig. 5G-I), it was not found oriented along the PD axis at this stage (not shown), whereas YFP-Rab11, YFP-Rab4, Hrs and Rab7 never accumulated at the cortex (not shown).

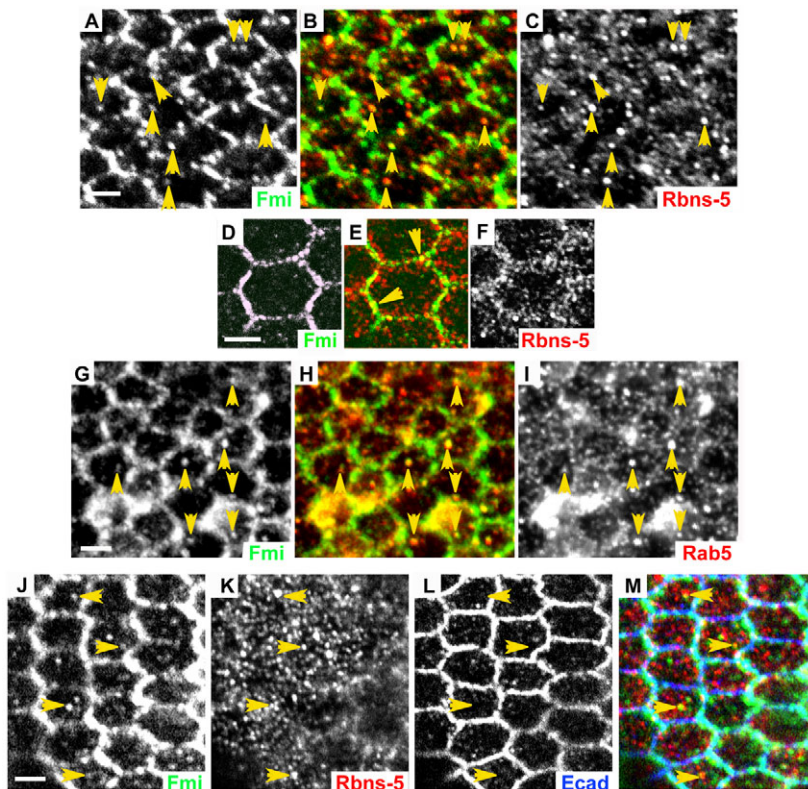


Fig. 5. Colocalization between Rbsn-5 and Fmi on endosomes and at the cortex. (A-F) Wild-type pupal wings at 26 (A-C) and 30 (D-F) hours APF at 25°C. Arrowheads indicate colocalization between Rbsn-5 (red) and Fmi (green). (G-I) Wild-type pupal wing at 26 hours APF at 25°C. Arrowheads indicate colocalization between Rab5 (green) and Fmi (red). (J-M) Wild-type pupal wing at 26 hours APF at 25°C. Arrowheads indicate colocalization between Rbsn-5 (red) and Fmi (green), but not E-Cad (blue). Single apical confocal sections are shown. Scale bar: 2.5 μ m.

When Fmi lost its polarized pattern (Usui et al., 1999) and hairs emerged and initiated outgrowth, Rbsn-5 became enriched in the distal part of the cell at the base of the emerging trichomes (Fig. 4N-P) and, later on, inside the trichomes (not shown).

These data show that during pupal wing development, Rbsn-5 displays a striking similarity with PCP proteins with respect to intracellular redistribution at the apical cell boundaries. Moreover, the relocation of Rbsn-5 at the base of the emerging trichomes together with the hair defects suggests a requirement for hair formation.

The PCP protein Flamingo colocalizes with Rbsn-5 in intracellular vesicles and at apical cell boundaries

During hexagonal packing and establishment of PCP, Fmi, together with Fz but not E-Cad, localizes in patches at the cortex and in endosomes (Classen et al., 2005; Shimada et al., 2006) (Fig. 4F). Interestingly, a fraction of Fmi vesicles in the apical side of the pupal wing epithelium colocalized with Rbsn-5 (Fig. 5A-C, arrowheads). Such colocalization progressively increased during hexagonal packing, with 66% of Fmi-positive vesicles being co-labelled for Rbsn-5 at 26-28 hours APF at 25°C, when the total number of Fmi intracellular vesicles detected increases (Shimada et al., 2006). At the same stage, Fmi vesicles were positive for Rab5 as well (Fig. 5G-I), suggesting that they correspond to early endosomes. These vesicles were labelled neither with E-Cad (Fig. 5J-M), nor YFP-Stbm (data not shown). In addition, Fmi also colocalized with Rbsn-5 on cortical punctuate structures, which might correspond to either endocytic vesicles or subdomains of the plasma membrane (Fig. 5D-F, arrowheads).

The colocalization with Fmi, the recruitment at apical cell boundaries concomitant with Fmi redistribution at the cortex and the PD polarity suggest that Rbsn-5 is linked to the intracellular trafficking of Fmi at the apical side of the pupal wing epithelium in the course of the establishment of PD polarity.

Flamingo, but neither Strabismus nor Frizzled, is rate limiting for the recruitment of Rbsn-5 at the apical cell boundaries

Fmi is required for the cortical membrane association of other PCP proteins (Axelrod, 2001; Rawls and Wolff, 2003; Shimada et al., 2001; Strutt, 2001; Usui et al., 1999). As Rbsn-5 colocalizes with Fmi, we investigated whether the cortical redistribution of Rbsn-5 is dependent on Fmi. In *fmi*¹⁹² null mutant clones at the time of PD polarization, Rbsn-5 no longer associated with the apical cortex, but appeared diffuse intracellularly (Fig. 6A-C). Overexpression of Fmi in pupal wings induced the accumulation of Rbsn-5 along the entire cortical domain where Fmi itself was also localized (Fig. 6D-F). Such Fmi-dependent recruitment of Rbsn-5 occurred regardless of the developmental stage and of the initial localization of Fmi and Rbsn-5 (see Fig. S4A-C in the supplementary material). The distribution of Rab5, however, was never affected by Fmi overexpression (not shown), indicating selectivity for Rbsn-5 localization at the cortex. Overexpression of other transmembrane PCP core proteins, such as Fz and Stbm, did not alter the intracellular distribution of Rbsn-5 in pupal wings (see Fig. S4D-I in the supplementary material), suggesting that only Fmi out of these proteins is rate limiting for the recruitment of Rbsn-5 at the cortex.

We next tested whether Fmi can interact directly with Rbsn-5. No interaction was observed between in vitro translated Rbsn-5 and the cytoplasmic tail of both Fmi isoforms (Fmi and Stan) so far described (Wasserscheid et al., 2007) in GST pull-down assays (data not shown). It remains possible that the recruitment of Rbsn-5 by Fmi might require an intermediate binding partner.

Rbsn-5 regulates intracellular trafficking of Fmi

Given its intracellular colocalization during hexagonal packing, we reasoned that Rbsn-5 could regulate internalization and recycling of Fmi. Indeed, loss of Rbsn-5 led to intracellular accumulation of

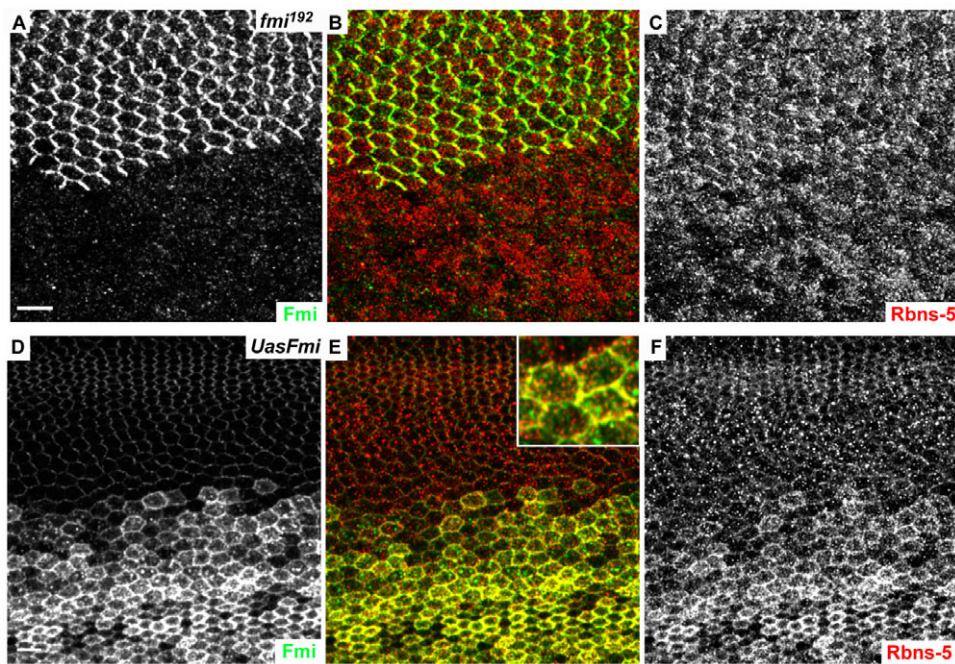


Fig. 6. Flamingo is rate limiting for the recruitment of Rbsn-5 at the apical cell boundaries of the pupal wing epithelium. (A-C) A *fmi*¹⁹² clone, defined by the loss of Fmi staining (green), in the pupal wing at 64 hours APF at 18°C stained for Rbsn-5 (red). Genotype is *y w/w hsp70-FLP;fmi*¹⁹²*FRT42/UbiGFP FRT42*. (D-F) A pupal wing at 26 hours APF at 25°C overexpressing Fmi (green) in the posterior compartment and stained for Rbsn-5 (red). Inset in E is a higher magnification view. Genotype is *w; en-gal4/Sp,UAS-Fmi/+*. Distal is right, proximal left. Scale bar: 10 μm.

the recycling Fmi fraction. Although the total amount of Fmi at the apical cell boundaries seemed unchanged (see Fig. S5A-D in the supplementary material), a fraction of Fmi was detected below the level of apical junctions in small cytoplasmic punctuate structures within the cells of *rbsn*³⁴ clones, but not in the surrounding wild-type cells (Fig. 7A,a-b; arrowheads). In *rbsn*³⁴ clones, we observed little colocalization between Fmi and Rab5 at the apical cell boundaries where Rab5 became strongly enriched (Fig. 7B,a-d). By contrast, we detected a partial colocalization with Hrs (Fig. 7B,e-h; arrowheads), and, to a lesser extent, with Rab7 (not shown), but no colocalization with the Golgi protein Lava lamp (not shown). These data are consistent with the established role of Rbsn-5 in transport to, and recycling from, endosomes (de Renzis et al., 2002). We cannot exclude that newly synthesized protein might contribute to the fraction of cytoplasmic Fmi. Nevertheless, the increased levels of endocytic markers, together with the partial colocalization of Fmi with Hrs and Rab7, suggest that endocytic trafficking is altered in *rbsn*³⁴ clones and that Fmi is mis-sorted to a late Hrs-positive compartment. The failure to recycle Fmi to the apical cell boundaries could explain why Fmi levels do not increase there, despite defects in endocytosis.

Consistent with recent data showing that during hexagonal packing Fmi is trafficked with Fz (Shimada et al., 2006; Strutt and Strutt, 2008), Fz accumulates sub-apically and colocalizes with Fmi on punctuate structures in *rbsn*³⁴ clones (Fig. 7C,a-d). By contrast, E-Cad did not accumulate in sub-cortical structures in *rbsn*³⁴ clones (see Fig. S5A-I in the supplementary material), ruling out a general defect in endocytic trafficking. Additionally, although at apical cell boundaries the distribution of the PCP proteins Dsh and Stbm was impaired as previously described (see Fig. S3 in the supplementary material), none of them accumulated sub-apically (see Fig. S5J-O in the supplementary material). These results suggest that Rbsn-5 specifically mediates the trafficking of Fmi.

As Rbsn-5 is a Rab5 effector, we next tested whether alterations of Rab5 activity could perturb Rbsn-5 association with the apical cell boundaries or endocytic trafficking of Fmi. Indeed, GFP-Rab5 overexpression at 30 hours at 25°C (Classen et al., 2008) shifted Rbsn-5 from the apical cell boundaries to Rab5-positive enlarged endosomes (Fig. 8E-H). In wings observed before the completion of hexagonal repacking and PCP polarization in the whole pupal wing (the stage when intracellular trafficking of Fmi was apparent in wild-type tissue), GFP-Rab5 overexpression could be seen to cause the accumulation of Fmi in enlarged early endosomes, where it colocalized with Rbsn-5 and GFP-Rab5 (Fig. 8A-D). When wings were observed at later stages, however, Fmi was normally polarized and no longer accumulated with overexpressed Rab5 (Fig. 8E-H). Furthermore, adult wings derived from these flies did not display trichome polarity defects (Fig. 8I). Interestingly, defects in planar polarization could be uncovered in Rab5 overexpressing adult wings when apoptosis was prevented by co-expression of p35 (Fig. 8J), a baculovirus-derived apoptosis inhibitor (Hay et al., 1994). Indeed, in pupal wings, GFP-Rab5 and p35 co-expression also caused the accumulation of Fmi and Rbsn-5 in GFP-Rab5 enlarged early endosomes (see Fig. S6A-D in the supplementary material). However, at later stages hexagonal packing was dramatically affected and the PD polarity of Fmi was lost (see Fig. S6E-G in the supplementary material). These data show that Rab5 overexpression alters Fmi trafficking, and causes planar polarization defects that are masked by apoptosis.

DISCUSSION

In the present study, we uncovered a novel role of Rbsn-5 in the establishment of PCP during pupal wing development, and we further demonstrated that the PCP protein Fmi undergoes endocytic trafficking in a process that is dependent on Rbsn-5 and required for the establishment of PCP.

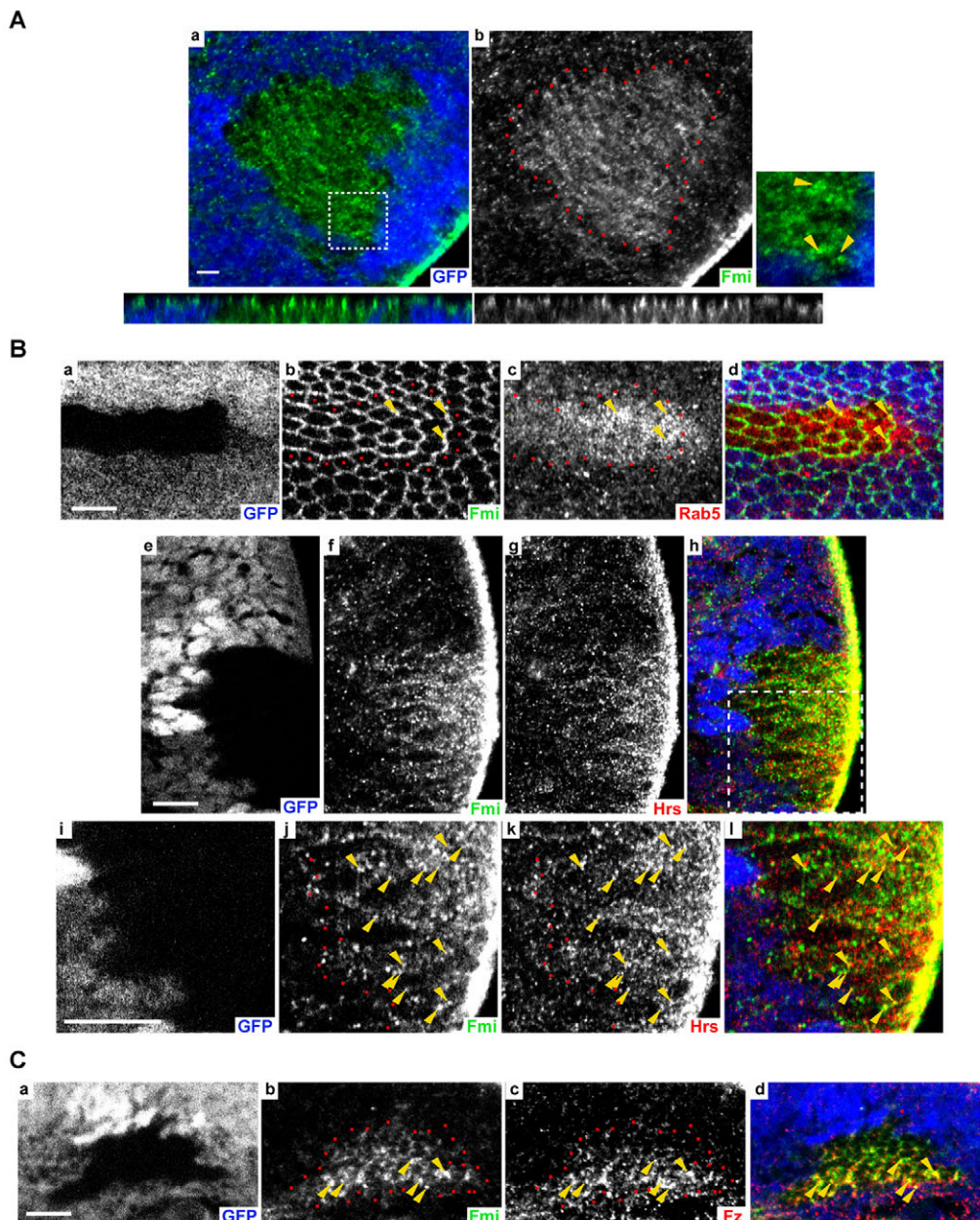


Fig. 7. Subapical accumulation of Flamingo in *rbsn³⁴* clones. *rbsn³⁴* clones, indicated by the absence of GFP (blue), in the pupal wing at 58 hours APF at 18°C. (Aa,b) Arrowheads indicate accumulation of Fmi (green) in vesicular structures (arrowheads). Panel on the right shows higher magnification of the area outlined in a. Panels below show an orthogonal view of the clone. (Ba-l) Arrowheads indicate colocalization between Fmi (green, b,d,f,h,j,i,l) and Rab5 (red, c,d) or Hrs (red, g,h,k,l). (i-l) Higher magnification of the area outlined in h. (Ca-d) Arrowheads indicate colocalization between Fmi (green, b,d) and Fz (red, c,d) in vesicular structures. Scale bar: 10 μm. Single confocal sections. Red dots indicate wild-type cells abutting the mutant clones. Distal is right, proximal left.

Rbsn-5 shares with its mammalian orthologue Rabenosyn-5 several structural features, as well as the function of molecular coordinator of endocytosis and recycling (de Renzis et al., 2002; Naslavsky et al., 2004). First, the inhibition of fluid-phase endocytosis observed in *rbsn³⁴* cells is consistent with the impairment of early endocytic transport described for both Rabenosyn-5 and Vps45 in mammalian cells, *C. elegans* and *Drosophila* (Gengyo-Ando et al., 2007; Morrison et al., 2008; Nielsen et al., 2000; Tanaka and Nakamura, 2008). Second, although Rbsn-5 does not bind Rab4, it interacts with EHD/RME1, a protein that is required for recycling cargo from endosomes to the surface (Grant et al., 2001; Lin et al., 2001; Naslavsky et al., 2004; Sommer et al., 2005). Third, the formation of expanded Rab5-positive endosomes in Rbsn-5 mutant cells phenocopies the endosomal enlargement observed upon inhibition of recycling (Cormont et al., 2001; Deneka et al., 2003). Moreover, the accumulation of Fmi in late endocytic compartments, which is also

consistent with the requirement of Rbsn-5 (and the yeast orthologue Vac1p) for protein sorting to the degradative pathway (Nielsen et al., 2000; Burd et al., 1997; Weisman and Wickner, 1992), resembles the phenotype previously described for *sec5^{E13}* clones in *Drosophila* oocytes (Sommer et al., 2005).

We found that the function of Rbsn-5 in endocytic transport is required for the re-distribution of Fmi between endosomes and the apical cell boundaries during the establishment of PCP in the *Drosophila* wing. Before PD asymmetry is established in the whole tissue, endogenous Fmi is detected on Rbsn-5- and Rab5-positive early endosomes. At later stages, Fmi must recycle back to the plasma membrane because it subsequently localizes to the apical cell boundaries concomitantly with Rbsn-5. Recycling from endosomes to the cell surface is also consistent with the dependence on Fmi for the recruitment of the exocyst subunit Sec5 at the apical cell boundaries (Classen et al., 2005). Loss of Rbsn-5 causes intracellular accumulation of Fmi, which correlates with

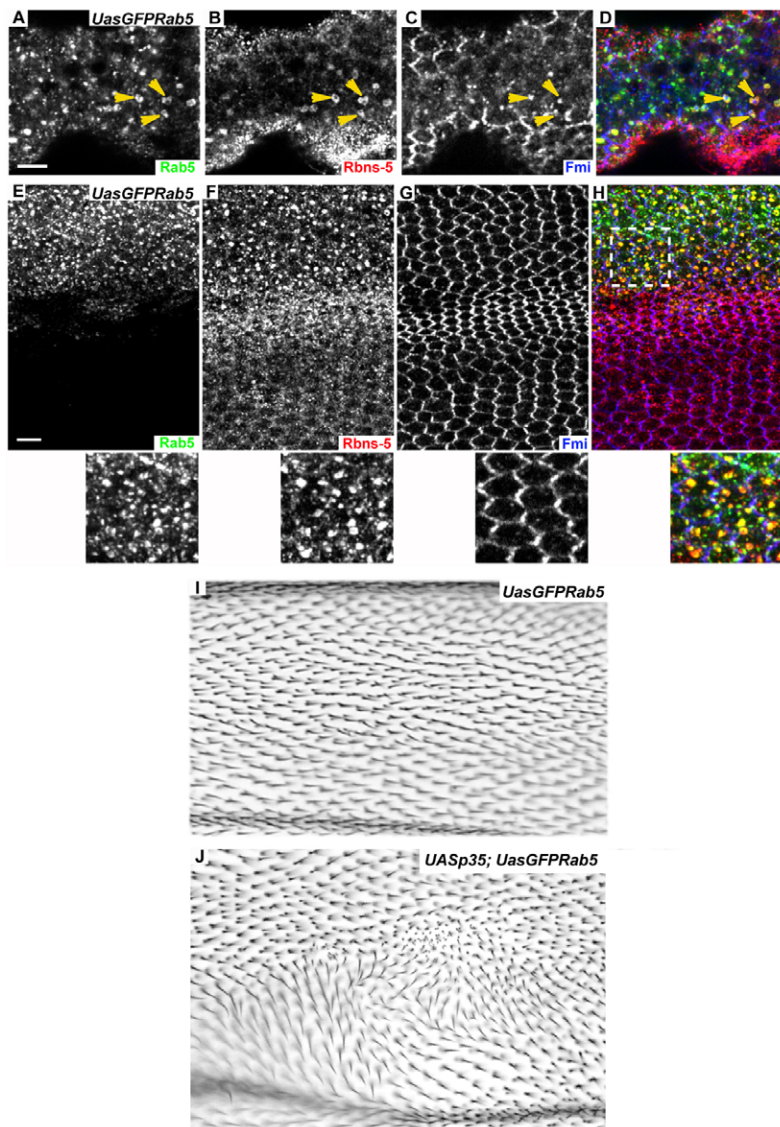


Fig. 8. Effect of GFP-Rab5 overexpression in the pupal wing on Fmi and Rbsn-5 localization.

(A-H) Pupal wing at 26 (A-D) and at 30 (E-H) hours APF at 25°C expressing GFP-Rab5 (green). Arrowheads indicate intracellular colocalization between GFP-Rab5, Rbsn-5 (red) and Fmi (blue). Apical confocal sections below the cortex (A-D) and projections of three apical confocal sections (E-H) are shown. Panels below show higher magnification of the wing area outlined in H. Genotype *ptc-gal4/UAS-GFP-Rab5*. Scale bar: 10 μm . (I, J) Adult wings overexpressing along the *ptc* domain GFP-Rab5 alone (I) or together with the baculovirus caspase inhibitor p35 (J). Distal is right, proximal left.

defects in PD polarity and hair orientation. Consistently, Rab5 overexpression, which influences Rbsn-5 redistribution, also alters Fmi trafficking and causes PCP defects. Our data therefore indicate that Rbsn-5-dependent trafficking of Fmi is relevant for the establishment of PCP. Clearly, our data do not exclude the possibility that other (e.g. biosynthetic) trafficking events of Fmi might contribute to this process.

Why is Fmi endocytosed and recycled during establishment of PCP in the pupal wing? It has been recently proposed that a combination of polarized secretion, Fmi endocytosis and stabilization of Fmi and Fz to the distal apical cell boundaries might underlie the establishment of cellular asymmetry (Shimada et al., 2006; Strutt and Strutt, 2008). In line with this proposal, Rbsn-5-dependent trafficking might be required to remove unstable Fmi (associating only to Fz) from the apical cell boundaries and relocate it in regions of the plasma membrane where it can be stabilized in proximal PCP complexes. Therefore, the weak proximal non-autonomy in trichome orientation observed for *rbsn*³⁴ clones, which resembles the phenotype of *fmi* clones rescued with a GFP-tagged Fmi mutant lacking the cytoplasmic domain [Fmi Δ intra-EGFP (Strutt and Strutt, 2008)], might be explained with the blockade of Fmi at the plasma membrane preferentially bound to Fz:Dsh complexes.

Some defects observed for *rbsn*³⁴ clones, such as Fmi redistribution as swirls and proximal perturbation of trichome polarity inside mutant clones, together with weak proximal non-autonomy are also reminiscent of defects in Fat and Ds mutant clones (Ma et al., 2003). Interestingly, we observed that big *rbsn*³⁴ clones could be found only on the distal side of the pupal wing. This might reflect a less important requirement for Rbsn-5 on this side compared with the proximal one. However, whether Rbsn-5 is also involved in the global propagation of PCP signalling via the upstream module Ds-Fat-Fj remains to be determined.

Additionally, Rbsn-5 mutant clones show defects in hair formation and elongation. As endocytosis and actin cytoskeleton remodelling are functionally connected (Lanzetti et al., 2001), these defects might be indirect consequences of endocytosis impairment. However, the specific accumulation of Rbsn-5 at the bottom of emerging hairs would be consistent with the idea that Rbsn-5 mediated endocytic/recycling trafficking might actively contribute to outgrowth of wing hairs, possibly by regulating specific membrane delivery.

While preparing this manuscript, a study on the regulation of membrane protein localization by PI3K (III) and Rabenosyn-5 in *Drosophila* wing cells reported (Abe et al., 2009) that loss-of-

function mutation of Rbsn-5 does not affect Fmi localization and hair formation and orientation. The discrepancy with our data could be explained by the fact that, in that study, the analysis was conducted at 25°C instead of 18°C. Indeed, we noticed that *rbsn*³⁴ clones are less healthy and tend to be smaller when grown at higher temperatures. Under these conditions, the intracellular accumulation of Fmi might well be less noticeable and the rate of lysosomal degradation may be higher.

In conclusion, the characterization of Rbsn-5 during *Drosophila* wing development allowed us to discover a novel function for this Rab5 effector in vivo in a developmental context and provided evidence in favor of a role of the apical endocytic trafficking of Fmi in the establishment of PCP. Future studies will hopefully provide additional molecular links and mechanistic insights into the functional interplay between the endocytic and the PCP machineries.

Acknowledgements

We are indebted to Drs Tadashi Uemura, Jeffrey D. Axelrod, Tanja Wolff, David Strutt, Hugo Bellen, Paul N. Adler and Elisabeth Knust for generously providing antibodies, constructs and fly stocks. The Flamingo #74 monoclonal antibody developed by T. Uemura and the rat anti-E-Cadherin developed by M. Takeichi were obtained from the Developmental Studies Hybridoma Bank, developed under the auspices of the NICHD and maintained by The University of Iowa, Department of Biological Sciences, Iowa City, IA 52242, USA. We thank Sven Sykora for excellent assistance with preparing transgenic flies, Angelika Giner for help with fly stocks, the Light Microscopy, Antibody and Protein Expression Facilities of the MPI-CBG for technical support, and Bianca Habermann for assistance in bioinformatic analysis. We thank Drs Elisabeth Knust, Stefano Bonatti, André Le Bivic and Manos Mavrikakis for helpful discussions and critical reading of the manuscript. We gratefully acknowledge the financial support of the Human Frontier Science Program Organization (G.M.), the Max-Planck Society, and grants from the E.U. (Endotrack), the BMBF and the DFG (M.Z.).

Competing interests statement

The authors declare no competing financial interests.

Supplementary material

Supplementary material for this article is available at <http://dev.biologists.org/lookup/suppl/doi:10.1242/dev.048413/-DC1>

References

- Abe, M., Setoguchi, Y., Tanaka, T., Awano, W., Takahashi, K., Ueda, R., Nakamura, A. and Goto, S. (2009). Membrane protein location-dependent regulation by PI3K (III) and rabenosyn-5 in *Drosophila* wing cells. *PLoS ONE* **4**, e7306.
- Adler, P. N. (2002). Planar signaling and morphogenesis in *Drosophila*. *Dev. Cell* **2**, 525-535.
- Adler, P. N., Krasnow, R. E. and Liu, J. (1997). Tissue polarity points from cells that have higher Frizzled levels towards cells that have lower Frizzled levels. *Curr. Biol.* **7**, 940-949.
- Axelrod, J. D. (2001). Unipolar membrane association of Dishevelled mediates Frizzled planar cell polarity signaling. *Genes Dev.* **15**, 1182-1187.
- Barbieri, M. A., Roberts, R. L., Gumusboga, A., Highfield, H., Alvarez-Dominguez, C., Wells, A. and Stahl, P. D. (2000). Epidermal growth factor and membrane trafficking. EGF receptor activation of endocytosis requires Rab5a. *J. Cell Biol.* **151**, 539-550.
- Bastock, R. and Strutt, D. (2007). The planar polarity pathway promotes coordinated cell migration during *Drosophila* oogenesis. *Development* **134**, 3055-3064.
- Bryant, N. J., Piper, R. C., Gerrard, S. R. and Stevens, T. H. (1998). Traffic into the prevacuolar/endosomal compartment of *Saccharomyces cerevisiae*: a VPS45-dependent intracellular route and a VPS45-independent, endocytic route. *Eur. J. Cell Biol.* **76**, 43-52.
- Bucci, C., Parton, R. G., Mather, I. H., Stunnenberg, H., Simons, K., Hoflack, B. and Zerial, M. (1992). The small GTPase rab5 functions as a regulatory factor in the early endocytic pathway. *Cell* **70**, 715-728.
- Burd, C. G., Peterson, M., Cowles, C. R. and Emr, S. D. (1997). A novel Sec18p/NSF-dependent complex required for Golgi-to-endosome transport in yeast. *Mol. Biol. Cell* **8**, 1089-1104.
- Christoforidis, S., McBride, H. M., Burgoyne, R. D. and Zerial, M. (1999). The Rab5 effector EEA1 is a core component of endosome docking. *Nature* **397**, 621-625.
- Classen, A. K., Anderson, K. I., Marois, E. and Eaton, S. (2005). Hexagonal packing of *Drosophila* wing epithelial cells by the planar cell polarity pathway. *Dev. Cell* **9**, 805-817.
- Classen, A. K., Aigouy, B., Giangrande, A. and Eaton, S. (2008). Imaging *Drosophila* pupal wing morphogenesis. *Methods Mol. Biol.* **420**, 265-275.
- Cormont, M., Mari, M., Galmiche, A., Hofman, P. and Le Marchand-Brustel, Y. (2001). A FYVE-finger-containing protein, Rabip4, is a Rab4 effector involved in early endosomal traffic. *Proc. Natl. Acad. Sci. USA* **98**, 1637-1642.
- de Renzis, S., Sonnichsen, B. and Zerial, M. (2002). Divalent Rab effectors regulate the sub-compartmental organization and sorting of early endosomes. *Nat. Cell Biol.* **4**, 124-133.
- Deneka, M., Neeft, M., Popa, I., van Oort, M., Sprong, H., Oorschot, V., Klumperman, J., Schu, P. and van der Sluijs, P. (2003). Rabaptin-5alpha/rabaptin-4 serves as a linker between rab4 and gamma(1)-adapin in membrane recycling from endosomes. *EMBO J.* **22**, 2645-2657.
- Eathiraj, S., Pan, X., Ritacco, C. and Lambright, D. G. (2005). Structural basis of family-wide Rab GTPase recognition by rabenosyn-5. *Nature* **436**, 415-419.
- Eaton, S. (2003). Cell biology of planar polarity transmission in the *Drosophila* wing. *Mech. Dev.* **120**, 1257-1264.
- Entchev, E. V., Schwabedissen, A. and Gonzalez-Gaitan, M. (2000). Gradient formation of the TGF-beta homolog Dpp. *Cell* **103**, 981-991.
- Gengyo-Ando, K., Kuroyanagi, H., Kobayashi, T., Murate, M., Fujimoto, K., Okabe, S. and Mitani, S. (2007). The SM protein VPS-45 is required for RAB-5-dependent endocytic transport in *Caenorhabditis elegans*. *EMBO Rep.* **8**, 152-157.
- Govel, J. P., Chavrier, P., Zerial, M. and Greenberg, J. (1991). rab5 controls early endosome fusion in vitro. *Cell* **64**, 915-925.
- Grant, B., Zhang, Y., Paupard, M. C., Lin, S. X., Hall, D. H. and Hirsh, D. (2001). Evidence that RME-1, a conserved *C. elegans* EH-domain protein, functions in endocytic recycling. *Nat. Cell Biol.* **3**, 573-579.
- Hay, B. A., Wolff, T. and Rubin, G. M. (1994). Expression of baculovirus P35 prevents cell death in *Drosophila*. *Development* **120**, 2121-2129.
- Hoepfner, S., Severin, F., Cabezas, A., Habermann, B., Runge, A., Gillooly, D., Stenmark, H. and Zerial, M. (2005). Modulation of receptor recycling and degradation by the endosomal kinesin KIF16B. *Cell* **121**, 437-450.
- Iwahashi, J., Kawasaki, I., Kohara, Y., Gengyo-Ando, K., Mitani, S., Ohshima, Y., Hamada, N., Hara, K., Kashiwagi, T. and Toyoda, T. (2002). *Caenorhabditis elegans* reticulon interacts with RME-1 during embryogenesis. *Biochem. Biophys. Res. Commun.* **293**, 698-704.
- Klein, T. J. and Mlodzik, M. (2005). Planar cell polarization: an emerging model points in the right direction. *Annu. Rev. Cell Dev. Biol.* **21**, 155-176.
- Lanzetti, L., Rybin, V., Malabarba, M. G., Christoforidis, S., Scita, G., Zerial, M. and Di Fiore, P. P. (2000). The Eps8 protein coordinates EGF receptor signalling through Rac and trafficking through Rab5. *Nature* **408**, 374-377.
- Lanzetti, L., Di Fiore, P. P. and Scita, G. (2001). Pathways linking endocytosis and actin cytoskeleton in mammalian cells. *Exp. Cell Res.* **271**, 45-56.
- Lin, S. X., Grant, B., Hirsh, D. and Maxfield, F. R. (2001). Rme-1 regulates the distribution and function of the endocytic recycling compartment in mammalian cells. *Nat. Cell Biol.* **3**, 567-572.
- Lloyd, T. E., Atkinson, R., Wu, M. N., Zhou, Y., Pennetta, G. and Bellen, H. J. (2002). Hrs regulates endosome membrane invagination and tyrosine kinase receptor signaling in *Drosophila*. *Cell* **108**, 261-269.
- Ma, D., Yang, C. H., McNeill, H., Simon, M. A. and Axelrod, J. D. (2003). Fidelity in planar cell polarity signalling. *Nature* **421**, 543-547.
- Marois, E., Mahmoud, A. and Eaton, S. (2006). The endocytic pathway and formation of the Wingless morphogen gradient. *Development* **133**, 307-317.
- Miaczynska, M., Christoforidis, S., Giner, A., Shevchenko, A., Uttenweiler-Joseph, S., Habermann, B., Wilm, M., Parton, R. G. and Zerial, M. (2004). APPL proteins link Rab5 to nuclear signal transduction via an endosomal compartment. *Cell* **116**, 445-456.
- Morrison, H. A., Dionne, H., Rusten, T. E., Brech, A., Fisher, W. W., Pfeiffer, B. D., Celniker, S. E., Stenmark, H. and Bilder, D. (2008). Regulation of early endosomal entry by the *Drosophila* tumor suppressors rabenosyn and Vps45. *Mol. Biol. Cell* **19**, 4167-4176.
- Mostov, K., Su, T. and ter Beest, M. (2003). Polarized epithelial membrane traffic: conservation and plasticity. *Nat. Cell Biol.* **5**, 287-293.
- Naslavsky, N., Boehm, M., Backlund, P. S., Jr and Caplan, S. (2004). Rabenosyn-5 and EHD1 interact and sequentially regulate protein recycling to the plasma membrane. *Mol. Biol. Cell* **15**, 2410-2422.
- Nielsen, E., Severin, F., Backer, J. M., Hyman, A. A. and Zerial, M. (1999). Rab5 regulates motility of early endosomes on microtubules. *Nat. Cell Biol.* **1**, 376-382.
- Nielsen, E., Christoforidis, S., Uttenweiler-Joseph, S., Miaczynska, M., Dewitte, F., Wilm, M., Hoflack, B. and Zerial, M. (2000). Rabenosyn-5, a novel Rab5 effector, is complexed with hVPS45 and recruited to endosomes through a FYVE finger domain. *J. Cell Biol.* **151**, 601-612.
- Oda, H., Uemura, T., Harada, Y., Iwai, Y. and Takeichi, M. (1994). A *Drosophila* homolog of cadherin associated with armadillo and essential for embryonic cell-cell adhesion. *Dev. Biol.* **165**, 716-726.

- Pal, A., Severin, F., Lommer, B., Shevchenko, A. and Zerial, M.** (2006). Huntingtin-HAP40 complex is a novel Rab5 effector that regulates early endosome motility and is up-regulated in Huntington's disease. *J. Cell Biol.* **172**, 605-618.
- Pevsner, J., Hsu, S. C., Hyde, P. S. and Scheller, R. H.** (1996). Mammalian homologues of yeast vacuolar protein sorting (vps) genes implicated in Golgi-to-lysosome trafficking. *Gene* **183**, 7-14.
- Raiborg, C., Bache, K. G., Mehlum, A. and Stenmark, H.** (2001). Function of Hrs in endocytic trafficking and signalling. *Biochem. Soc. Trans.* **29**, 472-475.
- Rawls, A. S. and Wolff, T.** (2003). Strabismus requires Flamingo and Prickle function to regulate tissue polarity in the Drosophila eye. *Development* **130**, 1877-1887.
- Saburi, S. and McNeill, H.** (2005). Organising cells into tissues: new roles for cell adhesion molecules in planar cell polarity. *Curr. Opin. Cell Biol.* **17**, 482-488.
- Shimada, Y., Usui, T., Yanagawa, S., Takeichi, M. and Uemura, T.** (2001). Asymmetric colocalization of Flamingo, a seven-pass transmembrane cadherin, and Dishevelled in planar cell polarization. *Curr. Biol.* **11**, 859-863.
- Shimada, Y., Yonemura, S., Ohkura, H., Strutt, D. and Uemura, T.** (2006). Polarized transport of Frizzled along the planar microtubule arrays in Drosophila wing epithelium. *Dev. Cell* **10**, 209-222.
- Sisson, J. C., Field, C., Ventura, R., Royou, A. and Sullivan, W.** (2000). Lava lamp, a novel peripheral golgi protein, is required for Drosophila melanogaster cellularization. *J. Cell Biol.* **151**, 905-918.
- Sommer, B., Oprins, A., Rabouille, C. and Munro, S.** (2005). The exocyst component Sec5 is present on endocytic vesicles in the oocyte of Drosophila melanogaster. *J. Cell Biol.* **169**, 953-963.
- Strigini, M. and Cohen, S. M.** (2000). Wingless gradient formation in the Drosophila wing. *Curr. Biol.* **10**, 293-300.
- Strutt, D. I.** (2001). Asymmetric localization of frizzled and the establishment of cell polarity in the Drosophila wing. *Mol. Cell* **7**, 367-375.
- Strutt, H. and Strutt, D.** (2005). Long-range coordination of planar polarity in Drosophila. *BioEssays* **27**, 1218-1227.
- Strutt, H. and Strutt, D.** (2008). Differential stability of flamingo protein complexes underlies the establishment of planar polarity. *Curr. Biol.* **18**, 1555-1564.
- Strutt, H. and Strutt, D.** (2009). Asymmetric localisation of planar polarity proteins: mechanisms and consequences. *Semin. Cell Dev. Biol.* **20**, 957-963.
- Tanaka, T. and Nakamura, A.** (2008). The endocytic pathway acts downstream of Oskar in Drosophila germ plasm assembly. *Development* **135**, 1107-1117.
- Tellam, J. T., James, D. E., Stevens, T. H. and Piper, R. C.** (1997). Identification of a mammalian Golgi Sec1p-like protein, mVps45. *J. Biol. Chem.* **272**, 6187-6193.
- Uemura, T. and Shimada, Y.** (2003). Breaking cellular symmetry along planar axes in Drosophila and vertebrates. *J. Biochem.* **134**, 625-630.
- Usui, T., Shima, Y., Shimada, Y., Hirano, S., Burgess, R. W., Schwarz, T. L., Takeichi, M. and Uemura, T.** (1999). Flamingo, a seven-pass transmembrane cadherin, regulates planar cell polarity under the control of Frizzled. *Cell* **98**, 585-595.
- van der Sluijs, P., Hull, M., Webster, P., Male, P., Goud, B. and Mellman, I.** (1992). The small GTP-binding protein rab4 controls an early sorting event on the endocytic pathway. *Cell* **70**, 729-740.
- Wasserscheid, I., Thomas, U. and Knust, E.** (2007). Isoform-specific interaction of Flamingo/Starry Night with excess Bazooka affects planar cell polarity in the Drosophila wing. *Dev. Dyn.* **236**, 1064-1071.
- Weisman, L. S. and Wickner, W.** (1992). Molecular characterization of VAC1, a gene required for vacuole inheritance and vacuole protein sorting. *J. Biol. Chem.* **267**, 618-623.
- Wucherpfennig, T., Wilsch-Brauninger, M. and Gonzalez-Gaitan, M.** (2003). Role of Drosophila Rab5 during endosomal trafficking at the synapse and evoked neurotransmitter release. *J. Cell Biol.* **161**, 609-624.
- Xu, T. and Rubin, G. M.** (1993). Analysis of genetic mosaics in developing and adult Drosophila tissues. *Development* **117**, 1223-1237.
- Yanagawa, S., van Leeuwen, F., Wodarz, A., Klingensmith, J. and Nusse, R.** (1995). The dishevelled protein is modified by wingless signaling in Drosophila. *Genes Dev.* **9**, 1087-1097.
- Zallen, J. A.** (2007). Planar polarity and tissue morphogenesis. *Cell* **129**, 1051-1063.
- Zerial, M. and McBride, H.** (2001). Rab proteins as membrane organizers. *Nat. Rev. Mol. Cell Biol.* **2**, 107-117.